

Analysis of the Creep Behavior of Polypropylene-Woodflour Composites

ADRIÁN J. NUÑEZ, NORMA E. MARCOVICH,
and MIRTA. I. ARANGUREN*

*INTEMA-Facultad de Ingeniería
Universidad Nacional de Mar del Plata
Juan B. Justo 4302, (7600) Mar del Plata, Argentina*

The creep behavior of composites prepared from woodflour and polypropylene has been analyzed. The woodflour content was varied from 0% to 60%. The compatibility between filler and matrix was varied by adding a non-commercial polypropylene-maleic anhydride copolymer (PPMAN) to the mixture. Short-term and long-term creep tests of woodflour/polypropylene composites at different temperatures were carried out. The effects of filler content, addition of compatibilizing agent and temperature were discussed. The creep deformation was generally reduced with woodflour addition, except at very high filler concentrations because of filler-wetting and dispersion problems. Low temperatures and addition of PPMAN also reduced the creep deformation. The creep compliance was modeled using the Burgers model and a power law equation. The parameters were found from the best fitting of experimental data using an optimization method. The Burgers model was found to provide a good description of the linear viscoelastic behavior. The mathematical description obtained from the short-term creep was utilized to predict the dynamic mechanical behavior of the composites with very good agreement between experimental and calculated values. Attempts to use the time-temperature-superposition principle to predict long-term creep from high temperature results were not successful because of the aging of the samples during creep at low temperatures. However, there was a good superposition of the short-term and long-term data at temperatures close to 70°C–80°C. The reason for this behavior is a relaxation of the PP matrix that takes place in that temperature range and erases any previous aging of the material. *Polym. Eng. Sci.* 44:1594–1603, 2004. © 2004 Society of Plastics Engineers.

INTRODUCTION

The use of natural fibers as reinforcement of polymeric matrices has attained great academic and commercial interest in the past decade owing to the low cost, large availability and biodegradability of the fibers. Wood fibers have low specific gravity, high specific strength and stiffness and they suffer little damage during processing. On the other hand, polypropylene (PP) is a versatile, recyclable, commodity polymer. Reinforced PP exhibits several attractive mechanical properties through an appropriate compounding of polymer and filler, allowing its use in several industrial sectors, such as automotive components, domestic appliances, frames, furniture and packaging. Because of its ease of processing, a large variety of shapes can be obtained.

Thus, PP-woodflour composites are increasing their market share because of their low cost and good mechanical properties and because of their environmentally friendly characteristics.

However, some disadvantages are associated with the use of natural fibers as reinforcements of polymers, such as their hygroscopicity and the incompatibility between lignocellulosic materials and polymer matrices, which lead to poor dispersion levels and low mechanical properties. In cellulosic-based materials, the hydrogen bonding tends to hold the cellulose fibrils together, which adversely affects the dispersion in a non-polar matrix. The dispersion and adhesion between the hydrophobic PP and hydrophilic woodflour can be improved by matrix modifications, fiber surface treatments or addition of a compatibilizing agent (1–4). In order to obtain a composite with competitive mechanical properties, a strong interface adhesion is required. Felix and Gatenholm (5) carried out the esterification of cellulose fibers with maleic anhydride (MAN) and MAN grafted

*To whom correspondence should be addressed. E-mail: marangur@fi.mdp.edu.ar
© 2004 Society of Plastics Engineers
Published online in Wiley InterScience (www.interscience.wiley.com).
DOI: 10.1002/pen.20157

polypropylene, and they observed a more effective wetting of the fibers by the PP matrix, leading to an improvement in the interfacial adhesion. Other authors have also observed this improvement when using commercial PPMAN copolymers as compatibilizers (6–8).

In recent years considerable work has been carried out to determine the mechanical properties of treated and untreated wood fiber–PP composites (8–12) such as tensile strength, Young's modulus, elongation at break and impact strength. However, little attention was given to their load-bearing abilities (13, 14). When considering composite materials with long-term application, their creep performance needs to be established. Polymers used in engineering applications are often subjected to stress for prolonged periods of time and used at high temperature, but it is not possible to know how a polymer will respond to a particular load without a detailed knowledge of its viscoelastic properties. Creep is the progressive deformation of a material at a constant load. The material suffers an instantaneous elastic deformation followed by a rapid creep rate decrease with time. Then, the creep rate reaches a steady-state value and finally, the creep rate increases rapidly and the material fractures. Accurate creep predictions are important especially in structural application of wood fiber/thermoplastic composites (14).

Numerous mathematical expressions and models have been proposed to describe creep behavior of polymers. Among these have been several attempts to develop constitutive methods to describe their nonlinear creep behavior. The most widely used nonlinear viscoelastic models are the Schapery model and its modifications, which are based on irreversible thermodynamics principles and have shown to accurately describe creep performance (15, 16). On the other hand, if the material is tested in the linear viscoelastic range, its creep behavior can be represented by simple rheological models. The Burgers model, which is a combination of elastic and viscous elements, has been reported to give a satisfactory representation of the creep compliance (17–19).

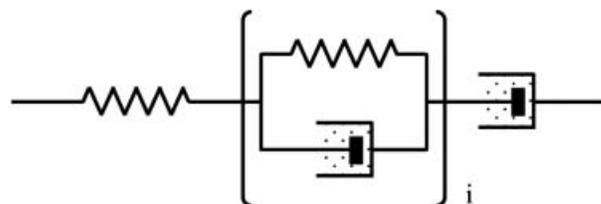
Long-term creep behavior might be predicted from short-term test data if the time-temperature-superposition principle is applicable to the studied material. Thus, master curves can be constructed to obtain information over a longer period of time than the experimental interval covered by the test. Differences between experimental long-term data and master curves may be attributed to "physical aging." This effect has been carefully studied for neat polypropylene by Tomlins and Read (20, 21). This aging process has been reported for room temperature experiments of long duration, even when it occurs well above the glass transition temperature of the material. While the aging process in completely amorphous materials is associated with the molecular activity below the glass transition, in semicrystalline polymers it is reported to reflect changes in the conformation of the tie molecules, which are part of the crystal lamellae (22). Increases in density and modulus are the consequent measurable changes in the

polymer (23). The whole process can be observed as a broad relaxation that has a maximum at about 80°C (α transition). Tomlins (22) has reported that heating PP at this temperature erases any previous aging effect.

The aim of this work is to investigate the creep performance of woodflour-PP composites. As the stress-transfer in a fiber-plastic composite depends on the fiber-matrix interfacial force of interaction, the compatibility between them was varied by adding a non-commercial maleic anhydride-polypropylene copolymer (PPMAN) to the mixture. Thus, effects of variations of woodflour content, interfacial interactions and temperature on the composites creep performance were studied. The application of the time-temperature-superposition principle was investigated by constructing a master curve from short-term creep tests, in conditions where aging could be neglected. Finally, the viscoelastic behavior of the materials was modeled using mechanical analogies and the accuracy of the predictions was evaluated. The best fitting parameters for the Burgers model were further used to describe the dynamic mechanical behavior of the composites.

THEORETICAL BACKGROUND

The simplest way to simulate the combined viscous and elastic behavior of a material is the use of mechanical analogies that include viscous elements (dashpots) and elastic elements (springs). In order to simulate the creep behavior, a viscoelastic liquid model with multiple retardation or relaxation times is used. The Burgers model is a combination of Maxwell and Kelvin-Voigt models, as shown in the scheme below:



Although this model does not represent the polymer structure, it has the advantage of being described by a differential equation, whose response to an applied stress can be easily solved analytically, giving a relatively good description of the polymer behavior. The total strain, $\varepsilon_{(t)}$, is given by:

$$\varepsilon_{(t)} = \frac{\sigma}{E_0} + \sum_{i=1}^{n-1} \frac{\sigma}{E_i} \cdot \left[1 - \exp\left(-t \cdot \frac{E_i}{\eta_i}\right) \right] + \frac{\sigma}{\eta_n} \cdot t \quad (1)$$

where σ is the applied stress, t is the time, E_0 is related to the instantaneous elastic response of the material, E_i is the elastic modulus of the spring and η_i is the viscosity of the dashpot of the i th Kelvin-Voigt element. The ratio η_i/E_i , the relaxation time (τ_i) of the i th element, is a measure of the time required for the extension of the spring to its equilibrium length while retarded by the dashpot; thus, the summation represents the retarded response of the material (decreasing creep rate). Finally, the last viscous element of the Maxwell element largely

contributes to the region of steady state creep, where the viscous flow is the predominant behavior.

If the study of the behavior of the material is limited to the linear viscoelastic region (LVE), defined as the region where the material properties are functions of time only and not of the applied stress or strain, the creep compliance, $J(t)$, is given by:

$$J(t) = \frac{1}{E_0} + \sum_{i=1}^{n-1} \frac{1}{E_i} \cdot \left[1 - \exp\left(-\frac{t}{\tau_i}\right) \right] + \frac{1}{\eta_n} \cdot t \quad (2)$$

Strictly, $J(t)$ is generally used to represent the shear compliance of the material. In the present work, it is used to represent the flexural compliance of the material measured using a three-point bending geometry.

The parameters were found from the best fitting of experimental data using a nonlinear least-squares optimization algorithm (iterative Levenberg-Marquardt method, Refs. 22, 24).

Other authors have preferred to use a phenomenological function of $J(t)$ with time, as follows (19, 25):

$$J(t) = a + b \cdot t^c \quad (3)$$

where a and b and c are empirically determined parameters. Equation 3 is very simple and has fewer fitting parameters than the Bürgers model, but it presents the disadvantage of not being able to predict other material properties.

When a creep experiment has progressed for some time and the stress is suddenly removed, the strain decreases with time, along a course called creep recovery. The rate of this reverse deformation depends on the material viscoelastic properties. The recovery tests are important because they allow us to distinguish between viscoelastic solids and viscoelastic liquids, whether the material recovers completely or a residual deformation (permanent set) remains after unloading. In the linear viscoelastic region, the creep recovery behavior can be predicted using the Boltzmann Superposition Principle (17, 26); thus the creep recovery compliance predicted by the Bürgers model, $J_r(t)$, is given by:

$$J_r(t) = J(t_r) - \frac{1}{E_0} - \sum_{i=1}^{n-1} \frac{1}{E_i} \cdot \left[1 - \exp\left(-\frac{t-t_r}{\tau_i}\right) \right] \quad (4)$$

where $J(t_r)$ is the compliance value at the moment when the specimen is unloaded (t_r). The parameters obtained from fitting the creep part of the tests, $J(t)$, were utilized in this work to predict $J_r(t)$.

In order to predict long-term behavior from short-term measurements, it is generally assumed that the polymer does not change its structure with time, so the time-temperature-superposition (TTS) principle holds. The creep curves obtained at different temperatures are superposed by horizontal shifts along a logarithmic time scale ($\ln a_T$) to obtain a master curve. This master curve allows a long time-range prediction at the selected temperature. In the case of composite materials, this assumption cannot be taken as valid *a priori*, but instead its applicability should be investigated. Different authors have shown that the approach is viable in some composite systems (17, 27–29). If the shifts in

the TTS are thought to be a process of matching relaxation times, the shift factors, a_T , are given by:

$$a_T = \frac{\tau(T)}{\tau(T_0)} = \frac{\eta(T)}{\eta(T_0)} \quad (5)$$

where $\tau(T)$ are the corresponding material relaxation times at a given temperature T , T_0 is the reference temperature and $\eta(T)$ and $\eta(T_0)$ are the viscosities of the material at the temperatures T and T_0 .

The shift factors can be correlated with temperature using the Williams-Landel-Ferry (WLF) equation or the Arrhenius equation. The former equation is given by:

$$\log(a_T) = \frac{-C_1 \cdot (T - T_0)}{C_2 + (T - T_0)} \quad (6)$$

where C_1 and C_2 are constants and T_0 is the reference temperature.

On the other hand, the Arrhenius equation is:

$$\ln(a_T) = \frac{-E_a}{R} \cdot \left(\frac{1}{T} - \frac{1}{T_0} \right) \quad (7)$$

where E_a is an activation energy and R is the universal gas constant.

Finally, the use of the Bürgers model allows us to calculate the properties of the material in the LVE region under different test conditions. In particular, the dynamic mechanical response can be predicted as follows:

$$\begin{aligned} J'_{(\omega)} &= \frac{1}{E_0} + \sum_{i=1}^{n-1} \frac{E_i}{E_i^2 + (\eta_i \cdot \omega)^2} \\ J''_{(\omega)} &= \sum_{i=1}^{n-1} \frac{\eta_i \cdot \omega}{E_i^2 + (\eta_i \cdot \omega)^2} + \frac{1}{\eta_n \cdot \omega} \quad (8) \\ E'_{(\omega)} &= \frac{J'_{(\omega)}}{J'_{(\omega)^2} + J''_{(\omega)^2}} \quad E''_{(\omega)} = \frac{J''_{(\omega)}}{J'_{(\omega)^2} + J''_{(\omega)^2}} \\ \tan \delta &= \frac{E''_{(\omega)}}{E'_{(\omega)}} = \frac{J''_{(\omega)}}{J'_{(\omega)}} \quad (9) \end{aligned}$$

where ω is the frequency, J' and J'' are the storage and loss compliance respectively, and E' and E'' are the storage and loss modulus respectively, which in this work were measured using the dynamic mode with three-point bending geometry.

EXPERIMENTAL

Materials

Woodflour from Eucalyptus Saligna (Argentina) was used as reinforcing filler. Particles passed through a sieve of mesh 100 (Tyler series).

Polypropylene Moplen (Himont, Italy) was utilized as the polymeric matrix for all the composites. A copolymer of maleic anhydride and polypropylene, PPMAN containing 0.3% (by weight) of maleic anhydride (modified J 300, University of Simon Bolivar, Venezuela) was used as compatibilizing agent in some of the samples. The characteristics of the PP and the compatibilizer are reported in Table 1.

Table 1. Characteristics of the PP Homopolymer and the Compatibilizing Agent Utilized.

	ρ (g/cm ³)	MFI (g/10 min.)	T_m (°C)	T_g (°C)
PP	0.91	17.20 ± 1.3	163.5	9.72
PPMAN	0.82	6.60 ± 1.4	162.5	2.98

Sample Preparation

Untreated woodflours were mixed with polypropylene in an intensive mixer at 180°C for 10 minutes, with or without the addition of a low concentration of compatibilizing agent PPMAN. Small pieces from these mixtures were cut and placed into the mold. Plaques of the composites (6 mm thick, 60 mm diameter) were obtained by compression at 180°C and 5 tons for 15 minutes. The samples were air-cooled in the mold under pressure.

Mechanical Tests

Creep Tests

A Perkin-Elmer dynamic mechanical analyzer (DMA 7) was used in the short-time creep experiments (test duration = 30 minutes). The tests were carried out in the creep mode, using the three-point bending fixture with a specimen platform of 15 mm length. The sample dimensions were approximately 20 × 2 × 3 mm³ and the linear dimensions were measured up to 0.01 mm.

Long-term creep tests were carried out in a Shimadzu Authograph S-500C with thermostatic chamber and especially modified for the task (test duration = up to rupture of the material, 8 hours to more than 12 days). The sample dimensions were 60 × 13 × 2.5 mm³ and the specimen platform was 40 mm. In both tests, the applied stress was 10 MPa.

Dynamic Mechanical Tests

The same equipment and sample dimensions reported for the short-time creep tests were used. In these experiments, the storage modulus (E'), loss modulus (E'') and phase lag ($\tan\delta$) were obtained. The tests were carried out using the frequency scan mode. The static stress and dynamic stress were 10 MPa and 3 MPa, respectively.

RESULTS AND DISCUSSION

Determination of the Linear Viscoelastic Region (LVER)

To ensure working in the linear viscoelastic range, isochronous experiments must be carried out (17). From a set of creep curves obtained at different constant applied stresses, strain-stress plots were constructed at different selected times. The isochronous curves are found to be linear up to certain stress and strain levels. Figure 1 shows the 30-minute results for pure PP obtained from tests run at 20°C. From analysis of the isochronous tests for PP (the sample showing the largest creep deformation), a stress of 10 MPa was selected for testing all the samples.

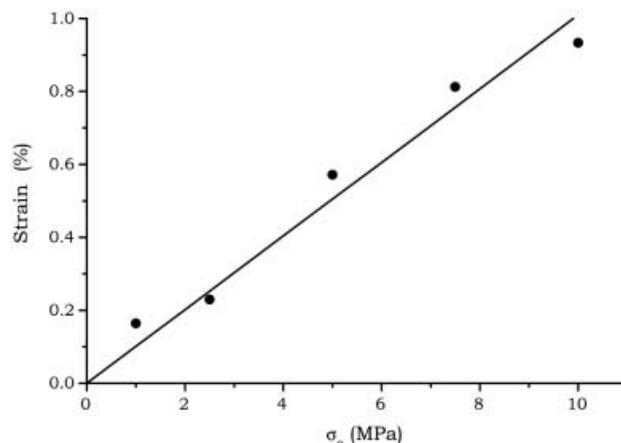


Fig. 1. Creep deformation (as %strain) of polypropylene after 30 minutes of applied load at 20°C.

Effect of Woodflour Addition

Composites made from semicrystalline thermoplastics and rigid fillers show a great variety of mechanical properties, depending on the composition and the processing conditions. The final properties of the composites are governed by the individual properties of the components as well as by the interactions developed at the matrix/filler interface. The effect of the addition of untreated woodflour to the PP matrix on the creep behavior at 20°C is shown in Fig. 2. As the filler concentration increases, the deformation decreases, as should be expected from the increased rigidity of the composites. The 60 wt% woodflour composite was an exception because the amount of filler is so high that the matrix does not wet the woodflour completely. The creep resistance is decreased by the presence of direct particle-particle interactions, which generate only physical or mechanical bonds, easily broken during deformation. Thus, the effect of the woodflour addition is the

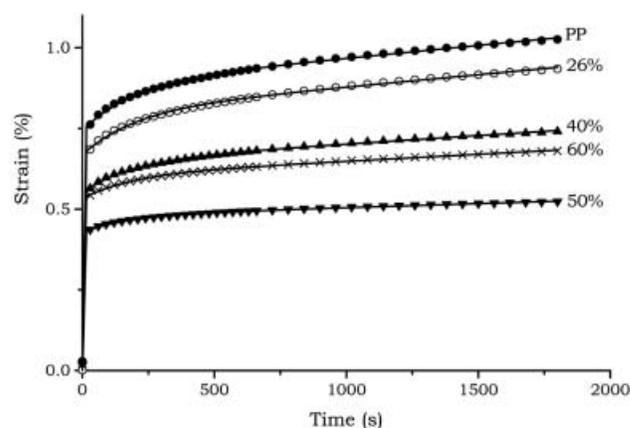


Fig. 2. Creep of the neat PP and untreated woodflour composites prepared with different filler concentrations at 20°C. Symbols are experimental data: ● Neat PP, ○ 26%, ▲ 40%, ▼ 50%, × 60%. Continuous lines correspond to the best fitting of the Burgers model with 4 parameters.

Table 2. Model Fitting Parameters. Composites Made From PP and Different Concentrations of Untreated Woodflour, at 20°C.

Sample	Bürgers Model				Power Law		
	E_0 (GPa)	E_1 (GPa)	η_1 (Pa·s)	η_n (Pa·s)	a	b	c
PP	1.35	6.85	1.33×10^{12}	1.27×10^{13}	5.96×10^{-10}	7.57×10^{-11}	0.232
26%	1.50	7.43	1.48×10^{12}	1.32×10^{13}	5.47×10^{-10}	5.91×10^{-11}	0.251
40%	1.82	10.12	1.92×10^{12}	1.92×10^{13}	4.44×10^{-10}	5.68×10^{-11}	0.220
50%	2.33	19.73	3.54×10^{12}	3.96×10^{13}	3.62×10^{-10}	3.88×10^{-11}	0.189
60%	1.88	13.75	2.55×10^{12}	2.32×10^{13}	4.69×10^{-10}	3.12×10^{-11}	0.255

stiffening of the composite, at least if filler wetting and dispersion are efficiently accomplished. Equation 2 with one Kelvin-Voigt element was used to fit the experimental data (four fitting parameters, $n = 2$). Table 2 includes the values of these parameters for the composites with different concentrations of woodflour, while continuous lines in Fig. 2 correspond to the model fits. As the filler percentage increases, the E_0 value increases (the immediate creep deformation decreases), as well as the steady state viscosity (the steady state creep decreases). This improvement in the rigidity of the material with the woodflour content, as well as the further deterioration at high loads, had been previously reported for woodflour composites using thermoplastic (8) and thermoset (30, 31) matrices.

Figure 3 illustrates the comparison of experimental results and the curves calculated using the power-law model. While both models result in a very good fit of the data, the power-law model is simpler to use and requires fewer fitting parameters (Table 2), although it does not offer possibilities of prediction of other LVE properties as the Bürgers model does.

Variation of the Interfacial Interactions

The effect of varying the adhesion between matrix and reinforcement, by addition of a compatibilizing agent, on the creep behavior was also analyzed. Figure 4 shows the creep behavior at 20°C for the different 40

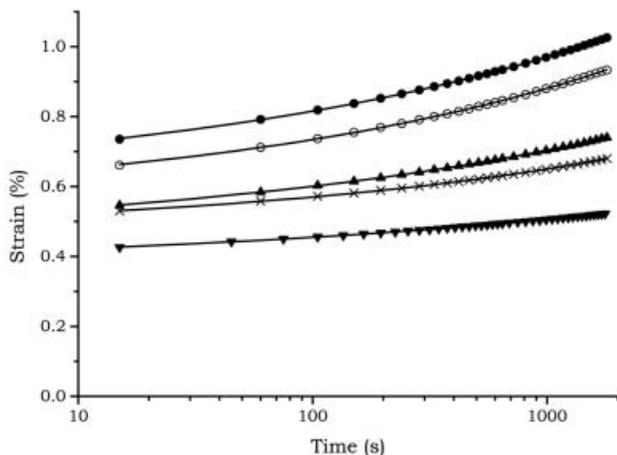


Fig. 3. Comparison of experimental and predicted creep using the power law model, for neat PP and untreated woodflour composites. Symbols have the same meaning as in Fig. 2. Continuous lines correspond to the best fitting of the Power Law Equation.

wt% woodflour composites prepared. All composites show less deformation with respect to the matrix at the same applied stress. The values of the Bürgers parameters are summarized in Table 3. An important reduction in creep deformation is observed when PPMAN compatibilizer is added to the formulation. The deformation decreases with increasing percentages of added PPMAN, as a result of the better dispersion of the particles during the mixing step and the improved final adhesion at the matrix-woodflour interphase (32). Samples prepared with 10 wt% of PPMAN showed a reduction of creep deformation of 45% compared to the matrix and 24% compared to the untreated composite at the end of the test. The creep deformation is further reduced when 10% instead of 5% of PPMAN is added to the PP-woodflour composites; although the main differences are seen between the 0% and 5% PPMAN added samples. Other authors have reported an optimum in the use of these types of additives (33, 34). The reason is that the compatibilizing agents are located in the interphase of the composites, and once the particles are completely wetted by the agent, no further improvement can be had by adding increasing amounts of the compatibilizer.

Creep and Creep Recovery

Creep behavior of a series of materials at 20°C was modeled using Eq 2 with one Kelvin-Voigt element. The fitting parameters were obtained from the creep experimental data, that is the initial 30 minutes, when the

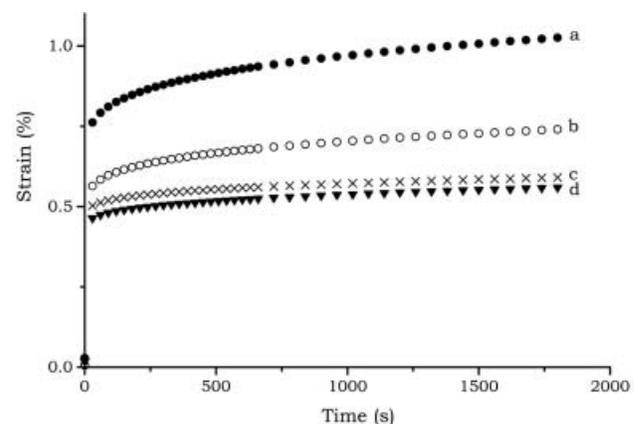


Fig. 4. Effect of the interfacial interactions on the creep behavior of the composites prepared with 40% woodflour. a) ● Neat PP, b) ○ Untreated Woodflour, c) × Untreated Woodflour and 5% PPMAN, d) ▼ Untreated Woodflour and 10% PPMAN.

Table 3. Model Fitting Parameters. Composites Made With 40% of Woodflour and Different Interfacial Modifiers at 20°C.

Sample	E_0 (GPa)	E_1 (GPa)	η_1 (Pa-s)	η_n (Pa-s)
Untreated WF	1.82	10.12	1.92×10^{12}	1.92×10^{13}
UWF + 5% PPMAN	2.02	20.73	3.67×10^{12}	3.68×10^{13}
UWF + 10% PPMAN	2.19	20.58	3.95×10^{12}	3.25×10^{13}

material is under loading ($\sigma_{\text{applied}} = 10$ MPa). These parameters were utilized in Eq 4 to predict the recovery part of the experiment (following 45 minutes). The fitting and prediction obtained with the model were generally excellent or at least very good, with the discrepancies with respect to the experimental data appearing in the recovery part of the curve, as shown in Fig. 5 for the composite containing 40% untreated woodflour and 10% PPMAN at 20°C. Although the model used is very simple, it is capable of representing the main features of the test during the loading and unloading parts of the creep test.

Effect of Temperature

In a partially crystalline polymer, the mobility of the amorphous tie molecules is greatly hindered by the reinforcing effect of the crystalline phase. The creep response, viscoelastic in nature, depends on the material structure, which is a strong function of the temperature of the test. In the range of temperatures analyzed, below the melting temperature, no changes in the crystallinity are expected. On the other hand, changes in the mobility of amorphous bulk and tie molecules occur. As the temperature increases, the mobility of the chains increases, and this results in increased creep deformation at the same applied stress (20, 21, 35). Note that for a given material, there are no changes in morphology (that is no changes in the crystallinity of the sample) but only those originated in the increased mobility of the chains at the higher temperatures.

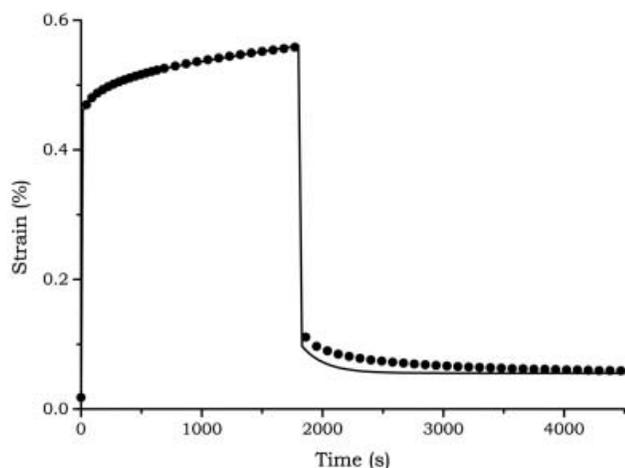


Fig. 5. Creep and creep recovery of the composite containing 40% untreated woodflour and 10% PPMAN. Filled circles are experimental points, continuous line is the Bürgers model calculation with one Kelvin-Voigt element (4-element model).

Figure 6 shows the strong temperature dependence of the creep behavior of the composite with 26 wt% of untreated woodflour. At the elapsed test time, the strain at 50°C and 80°C are 2.15 and 3.93 times the strain at 20°C, respectively. At 80°C, the creep curve reaches the last stage where the strain rate increases with time leading to the final material failure. This part of the curve was not included in the mathematical analysis, since nonlinear features would invalidate the use of the linear model. Table 4 includes the calculated values for the Bürgers fitting parameters corresponding to Fig. 6. E_0 and η_n values show a reduction with increasing temperature as a result of the material softening.

Time-Temperature Superposition and Long-Term Creep

The superposition technique exploits the sensibility of the molecular relaxation process to temperature. Under certain simplifying assumptions, a quantitative equivalence between time and temperature can be achieved. Thus, a long time experiment can be replaced by a shorter one at higher temperature. Although this technique cannot be assumed to be applicable *a priori* in multiphased systems, it has been shown to be effective in the characterization of different composite materials

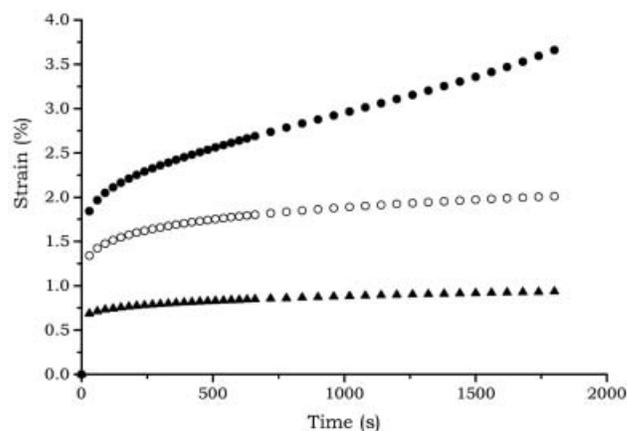


Fig. 6. Creep of the composites containing 26% of untreated woodflour at different temperatures. ● 80°C, ○ 50°C, ▲ 20°C.

Table 4. Model Fitting Parameters. Composites Made with 26% of Untreated Woodflour, at Different Temperatures.

T (°C)	E_0 (GPa)	E_1 (GPa)	η_1 (Pa-s)	η_n (Pa-s)
20°C	1.50	7.43	1.48×10^{12}	1.32×10^{13}
50°C	0.78	2.47	4.66×10^{11}	5.38×10^{12}
80°C	0.59	2.21	2.33×10^{11}	1.25×10^{12}

(17, 27–29). To predict long-term data, the creep compliance data at various temperatures were shifted according to the TTS principle. The reference temperature selected was 60°C. The “master curve” constructed from short-term data for the composite containing 40% untreated woodflour and 10% PPMAN (40 PPMAN) is shown in Fig. 7 and the horizontal shifts utilized for its construction are presented in Table 5. The shift values were correlated with temperature according to the WLF and Arrhenius equations (Eqs 6 and 7 respectively). The constants C_1 and C_2 of the WLF equation resulted equal to 11.46 and 137.43 respectively. The E_a/R value from the Arrhenius equation was 23.9×10^3 °K. Comparison of experimental values and WLF and Arrhenius models (Fig. 8) indicates a good match with any of the equations, although the WLF gives a slightly better fitting in the range of temperatures considered.

Although a “master curve” was successfully constructed, it is not a sufficient condition to validate the TTS principle. One reason for the occasional differences found between experimental data and master curves is physical aging (17, 35–37). In completely amorphous polymers, the glass rubber transition occurs in a relatively narrow temperature range, below which aging occurs. This is not the case in semicrystalline polymers, where the amorphous fractions close to the crystalline regions contain chains that may be partially incorporated in both phases and consequently are strongly hindered in their mobility. These chains require a significantly higher activation energy for relaxation. The result is that the transition for these polymeric fractions is expanded towards higher temperatures. Thus, for polypropylene, aging can take place at room temperature, and can be effectively erased by heating the sample at temperatures near 80°C. Pioneer work had already detected changes in polypropylene properties at room temperature; the studies showed no changes in the crystallinity of the samples, but a steadily increasing density. Gas sorption and diffusion experiments

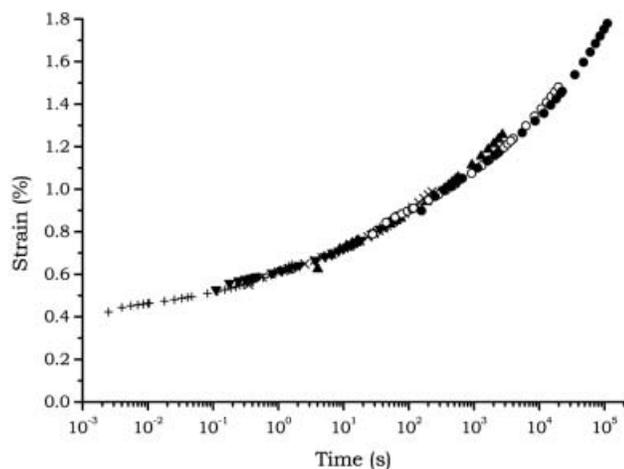


Fig. 7. Master curve constructed from the short-term creep data for the 40 PPMAN composite. The reference temperature is 60°C. ● 80°C, ○ 70°C, ▲ 60°C, × 50°C, ▼ 40°C, + 30°C.

Table 5. Shift Factor Values for Short-Term Creep Tests for 40 PPMAN Composite.

T (°C)	log a_T
30	3.30
40	1.65
50	1.15
60	0.00
70	-0.75
80	-1.50

allowed identification of the amorphous phase as the responsible for these changes (Refs. 11–13 and 19 in Fiebig *et al.* (23)).

Thus, if aging takes place during creep it would result in a lower than expected compliance. Differences in physical aging taking place during the experiment can be neglected in the short-term tests, because of the short length of time involved. On the other hand, during long-term tests, the material can suffer physical aging while the material creeps. Thus, the “master curve” obtained from short-term creep data may not represent the experimental behavior of the composite for long-term creep.

Experimental long-term creep tests (40 PPMAN samples) were carried out up to the rupture of the material, which occurred at >11.7 days at 50°C (the sample did not break before the end of the test), 6.87 days at 60°C, 2.14 days at 70°C and 8.17 hours at 80°C. The results are shown in Fig. 9.

If aging had not affected the long-term creep test, the a_T values tabulated in Table 5 could have been used to construct a master curve, which should be superposable on the one obtained from the short-term data. Fig. 10 shows the experimental data for the long-term creep tests shifted according to the a_T values already reported (Table 5), where the line represents the short-term creep “master curve,” included for comparison. The reference temperature is 60°C in both cases. At

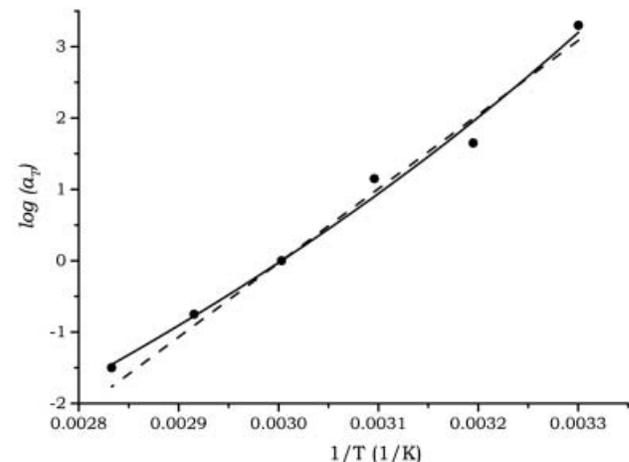


Fig. 8. Experimental shifts ($\log a_T$) used in the construction of the creep master curve and calculated shift corrections using the WLF and the Arrhenius equations (Eqs 7 and 8). (filled circles) Experimental, — WLF, --- Arrhenius.

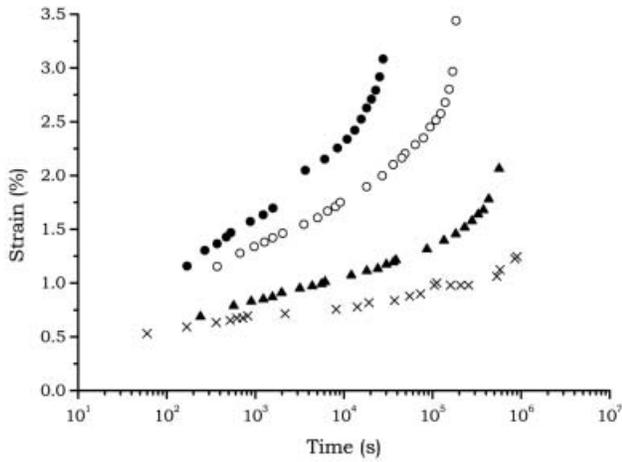


Fig. 9. Long-term creep of 40 PPMAN composites at different temperatures. Symbols have the same meaning as in Fig. 7.

temperatures below the α transition (50°C and 60°C), the creep test lasted many days, aging took place, and a mismatch between the predicted and the actual behavior is observed. At these temperatures, the material behaved more rigidly, in agreement with the expected changes (ex: increasing modulus). On the other hand, there is a good superposition at 70°C and 80°C between the prediction and the experimental data. The reason is that in this range of temperatures, any previous aging is satisfactorily erased, as has been previously reported (21, 23, 38).

Prediction of Dynamic Mechanic Behavior

The dynamic mechanic behavior of the composite can be predicted using the parameters determined from the mechanical models, since in both cases aging can be

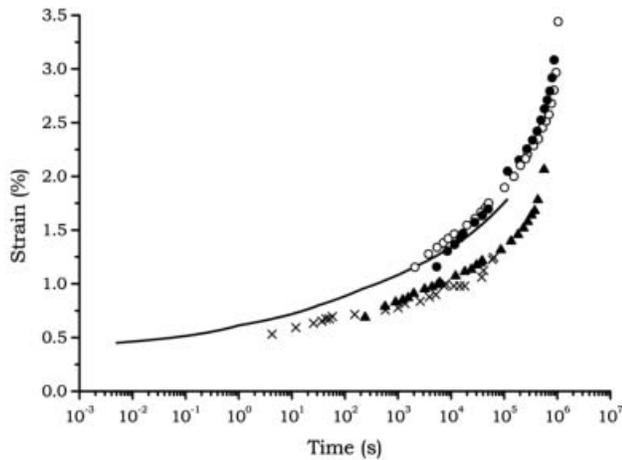


Fig. 10. Short-term master curve and results from long-term creep data. The shifts obtained from the short-term creep curves were also applied to the long-term creep data at the different temperatures; $T_{ref} = 60^\circ\text{C}$. Continuous line represents the calculated Burgers model with nine Kelvin-Voigt elements. Symbols have the same meaning as in Fig. 7.

Table 6. Parameter Values for the Burgers Model with Nine Kelvin-Voigt Elements Calculated From the Master Curve of the Composite Prepared With 40% WF and 10% PPMAN at $T_{ref} = 60^\circ\text{C}$. $\eta_n = 4.88 \times 10^{14}$ Pa·s, $E_0 = 2.01$ GPa.

<i>ith</i> element	λ_i (s)	E_i (GPa)
1	5	9.37
2	10	9.01
3	50	13.15
4	100	7.88
5	500	32.74
6	1000	5.82
7	5000	57.09
8	10,000	4.47
9	50,000	4.51

neglected. Thus, the creep master curve at 60°C constructed from short-term data at different temperatures was also modeled with the Burgers model. The shape of the creep curve depends on the distribution of retardation times. As the master curve covers a long range of time, many retardation times were needed to obtain a good description of the retarded creep zone where the creep rate decreases with time. The retardation times related to the Kelvin-Voigt elements were fixed at 5, 10, 50, 100, 500, 1000, 5000, 10,000, 50,000 seconds, while E_0 , E_i and η_n were the fitting parameters. Again, the Burgers model accurately depicts the viscoelastic behavior. The fitting parameters utilized are shown in Table 6.

The dynamic mechanical response of the material was calculated using Eqs 8 and 9 and the best fitting parameters obtained for the Burgers model from the creep master curve at 60°C. To obtain the dynamic mechanical prediction at a different temperature (70°C), the relaxation times used in modeling the 60°C-master curve were corrected with Eq 5, using the corresponding shift factor ($\log a_T = -0.75$). Fig. 11 shows the comparison between predicted and experimental results.

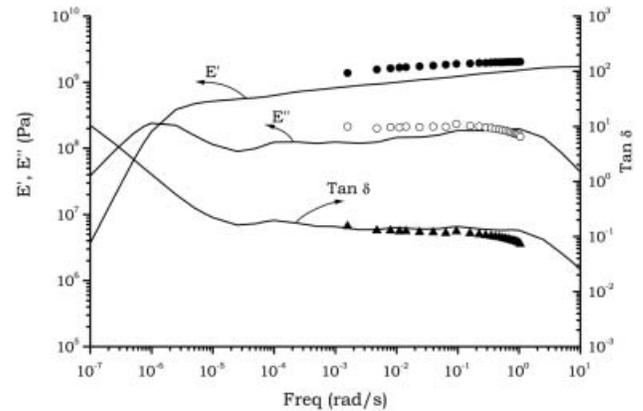


Fig. 11. Dynamic mechanical behavior of the 40 PPMAN composite at 70°C. Points are experimental data; continuous lines are the curves calculated (Eqs 8 and 9) from the results of modeling the creep master curve at 60°C and using the corresponding shift in the calculus of the effective times. ● E' , ○ E'' , ▲ $\text{Tan } \delta$.

The good agreement observed demonstrates the reliability of the model and the applicability of the TTS principle to the non-aged system. The use of the Burgers model with multiple Kelvin-Voigt elements applied to the creep master curve was needed to represent the material behavior. The use of the simplest model with only one Kelvin-Voigt element predicts an inflexion in $\tan \delta$ (a very short plateau at $\tan \delta = 0.1$), but since it includes only one relaxation time, it is unable to predict the wide transition observed experimentally. This problem was solved considering multiple time relaxations (a discrete retardation spectrum was utilized). It could have also been solved, although with increased mathematical complexity, using a continuous retardation spectrum. Although the set of fitting parameters in the retarded creep zone is obviously arbitrary, once they are determined from fitting a LVE test, they can be used to predict the LVE behavior of the material under different stress conditions, as was demonstrated in this work.

CONCLUSIONS

The effects of woodflour content, interface treatments, and temperature on the creep behavior of woodflour-PP composites were studied. In some cases a compatibilizer, PPMAN, was added to the mixture. The results show that the creep deformation is decreased when the woodflour concentration was increased, except when it was too high to achieve a complete wetting and good dispersion of the particles in the matrix. The addition of a small amount of PPMAN to the mixture greatly improved the creep behavior, probably because of the improved compatibility and the development of a stronger interface. Temperature is an important parameter when designing composites for applications, as polymers soften when temperature is increased.

The Burgers model was able to represent the viscoelastic behavior of the woodflour-PP composites. The model with one Kelvin-Voigt element is enough to fit adequately the creep and creep recovery of the materials for short-term tests. On the other hand, the simpler power law model gives a good fit at short times, although it is not flexible enough as to be used in the prediction of LVE dynamic mechanical tests.

Several Kelvin-Voigt elements in the Burgers model were needed to fit the master curve and to predict correctly the dynamic mechanical behavior of the composites. The agreement of the experimental data from creep recovery and dynamic mechanical tests with the calculated values shows that the Burgers model including a distribution of relaxation times is a simple but powerful tool to represent the viscoelastic response of the polymer and composites studied.

Master curves constructed from short-term creep data did not accurately depict the long-term real behavior of the materials at low temperatures. However, there was a good superposition of the short-term and long-term data at temperatures in the range of 70°C to 80°C, where a process of molecular relaxation takes place. This process results in the "rejuvenation" of the material.

ACKNOWLEDGMENTS

The authors thank CONICET (National Research Council, Argentina) for the financial support to the project and the fellowship awarded to one of the authors (A. Nuñez).

REFERENCES

1. K. Bledzki and J. Gassan, *Progress in Polymer Science*, **24**, 221–74 (1999).
2. S. J. Eichhorn, C. A. Baillie, N. Zafeiropoulos, L. Y. Mwaikambo, M. P. Ansell, A. Dufresne, K. M. Entwistle, P. J. Herrera-Franco, and G. C. Escamilla, *J. Materials Science*, **36**, 2107–31 (2001).
3. J. George, M. S. Sreekala, and S. Thomas, *Polym. Eng. Sci.*, **41**, 1471 (2001).
4. R. Gauthier, C. Joly, A. C. Copuas, H. Gauthier, and M. Escoubes, *Polym. Compos.*, **19**, 287 (1998).
5. J. M. Felix and P. Gatenholm, *J. Applied Polymer Science*, **42**, 609–20 (1991).
6. M. Kazayawoko, J. J. Balatinez, and L. M. Matuana, *J. Materials Science*, **34**, 6189–99 (1999).
7. J. Gassan and A. K. Bledzki, *Composites Part A*, **28A**, 1001–05 (1997).
8. M. N. Ichazo, C. Albano, J. González, R. Perera, and M. V. Candal, *Composite Structures*, **54**, 207–14 (2001).
9. M. N. Anglès, J. Salvadó, and A. Dufresne, *J. Applied Polymer Science*, **74**, 1962–77 (1999).
10. K. Oksman and C. Clemons, *J. Applied Polymer Science*, **67**, 1503–13 (1998).
11. X. Chen, Q. Guo, and Y. Mi, *J. Applied Polymer Science*, **69**, 1891–99 (1998).
12. J. Wu, D. Yu, C.-M. Chan, J. Kim, and Y.-W. Mai, *J. Applied Polymer Science*, **76**, 1000–10 (2000).
13. M. M. Sain, J. Balatinez, and S. Law, *J. Applied Polymer Science*, **77**, 260–68 (2000).
14. B.-D. Park and J. J. Balatinez, *Polym. Compos.*, **19**, 377 (1998).
15. T. W. Strganac and H. J. Golden, *Int. J. Solid Structures*, **33(30)**, 4561–70 (1996).
16. J. G. J. Beijer and J. L. Spoomaker, *Computers and Structures*, **80**, 1213–29 (2002).
17. C. Marais and G. Villoutreix, *J. Applied Polymer Science*, **69**, 1983–91 (1998).
18. M. Frounchi, *J. Applied Polymer Science*, **64**, 971–82 (1997).
19. J. P. Lu, L. S. Burn, and B. E. Tiganis, *Polym. Eng. Sci.*, **40**, 2407 (2000).
20. B. E. Read and P. E. Tomlins, *Polym. Eng. Sci.*, **37**, 1572 (1997).
21. P. E. Tomlins and B. E. Read, *Polymer*, **39**, 355–67 (1998).
22. P. E. Tomlins, *Polymer*, **37**, 3907–3913 (1996).
23. J. Fiebig, M. Gahleitner, C. Paulik, and J. Wolfschwenger, *Polymer Testing*, **18**, 257–66 (1999).
24. W. Marquardt, *SIAM J.*, **11**, 431 (1963).
25. W. J. Liou and C. I. Tseng, *Polym. Compos.*, **18**, 492 (1997).
26. J. D. Ferry, *Viscoelastic Properties of Polymers*, Wiley and Sons, New York (1980).
27. V. P. Cyras, J. F. Martucci, S. Iannace, and A. Vázquez, *J. Thermoplastic Composite Materials*, **15**, 253–65 (2002).
28. A. Vázquez, V. A. Dominguez, and J. M. Kenny, *J. Thermoplastic Composite Materials*, **12**, 253–65 (1999).
29. M. Sumita, T. Shizuma, K. Miyasaka, and K. Ishikawa, *J. Macromol. Sci.-Phys.*, **B22(4)**, 601–18 (1983).
30. N. Marcovich, M. Aranguren, and M. Reboredo, *Polymer*, **42**, 815–25 (2001).
31. N. Marcovich, M. Aranguren, and M. Reboredo, *J. Applied Polymer Science*, **70**, 2121–31 (1998).
32. A. J. Nuñez, P. C. Sturm, J. M. Kenny, M. I. Aranguren, N. E. Marcovich, and M. M. Reboredo, *J. Applied Polymer Science*, **88**, 1420–28 (2003).

33. B. Pukánszky, F. Tüdüs, J. Jancar, and J. Kolaric, *J. Materials Science Letters*, **8**, 1040–42 (1989).
34. S. Takase and N. Shiraishi, *J. Applied Polymer Science*, **37**, 645–59 (1989).
35. D. S. Matsumoto, *Polym. Eng. Sci.*, **28**, 1313 (1988).
36. D. Dean, M. Husband, and M. Trimmer, *J. Polymer Science B: Polymer Physics*, **70**, 2971–79 (1998).
37. L. C. Brinson and T. S. Gates, *Int. J. Solid Structures*, **32(6/7)**, 827–46 (1995).
38. A. J. Nuñez, J. M. Kenny, M. M. Reboredo, M. I. Aranguren, and N. E. Marcovich, *Polym. Eng. Sci.*, **42**, 733 (2002).